



Integration of Moran's I, geographically weighted regression (GWR), and ordinary least square (OLS) models in spatiotemporal modeling of COVID-19 outbreak in Qom and Mazandaran Provinces, Iran

Vahid Isazade¹ · Abdul Baser Qasimi² · Pinliang Dong³ · Gordana Kaplan⁴ · Esmail Isazade⁵

Received: 13 December 2022 / Accepted: 24 January 2023 / Published online: 15 February 2023
© The Author(s), under exclusive licence to Springer Nature Switzerland AG 2023

Abstract

Globally, the COVID-19 pandemic is a top-level public health concern. This paper attempts to identify the COVID-19 pandemic in Qom and Mazandaran provinces, Iran using spatial analysis approaches. This study was based on secondary data of confirmed cases and deaths from February 3, 2020, to late October 2021, in two Qom and Mazandaran provinces from hospitals and the website of the National Institute of Health. In this paper, three geographical models in ArcGIS 10.8.1 were utilized to analyze and evaluate COVID-19, including geographic weight regression (GWR), ordinary least squares (OLS), and spatial autocorrelation (Moran I). The results from this study indicate that the rate of scattering of confirmed cases for Qom province for the period was 44.25%, while the rate of dispersal of the deaths was 4.34%. Based on the GWR and OLS model, Moran's statistics demonstrated that confirmed cases, deaths, and recovered followed a clustering pattern during the study period. Moran's Z-score for all three indicators of confirmed cases, deaths, and recovered was confirmed to be greater than 2.5 (95% confidence level) for both GWR and OLS models. The spatial distribution of indicators of confirmed cases, deaths, and recovered based on the GWR model has been more scattered in the northwestern and southwestern cities of Qom province. Whereas the spatial distribution of the recoveries of the COVID-19 pandemic in Qom province was 61.7%, the central regions of this province had the highest spread of recoveries. The spatial spread of the COVID-19 pandemic from February 3, 2020, to October 2021 in Mazandaran province was 35.57%, of which 2.61% died, according to information published by the COVID-19 pandemic headquarters. Most confirmed cases and deaths are scattered in the north of this province. The ordinary least squares model results showed that the spatial dispersion of recovered people from the COVID-19 pandemic is more significant in the central and southern regions of Mazandaran province. The Z-score for the deaths Index is more significant than 14.314. The results obtained from this study and the information published by the National Headquarters for the fight against the COVID-19 pandemic showed that tourism and pilgrimages are possible factors for the spatial distribution of the COVID-19 pandemic in Qom and Mazandaran provinces. The spatial information obtained from these modeling approaches could provide general insights to authorities and researchers for further targeted investigations and policies in similar circumstances.

Keywords COVID-19 · Geographically weighted regression · Least squares model · Spatial autocorrelation · Qom · Mazandaran

Introduction

Coronavirus (SARS-COV-2)-related viral pneumonia with an unidentified agent was reported in Wuhan, China, toward the end of December 2019 (Comito and Pizzuti 2022). As

a result of the virus' rapid global spread and border crossings, 196 countries were afflicted on March 25, 2020. (Lu et al. 2020). The virus is an organ of the coronavirus family of the order Nidovirales and is a giant single-stranded RNA virus (Wang et al. 2010). The United Nations has explained COVID-19 as a leading social, human, and economic catastrophe that affects even developed countries; continuing the outbreak of this pandemic will cause problems for the global health community system, which will result in a population crisis of the world (Mollalo et al. 2020; Wu et al. 2020).

✉ Abdul Baser Qasimi
qasimi.abdul.a@gmail.com; qasimi.abdul.a@smgu.edu.af

Extended author information available on the last page of the article

The outbreak and intensity of an infectious disease epidemic significantly depend on the “infectious power of the disease” (Bailey and Gatrell 2015; Kandwal et al. 2009). In order to assess the risk of COVID-19 and identify areas that are now at high risk, all necessary information should be immediately available.

More than 185 countries being affected shows how quickly the coronavirus is spreading, necessitating cutting-edge technologies to evaluate the danger in particular areas. The spatial investigation of this pandemic virus can significantly benefit from using geographic information systems (GIS) (Zhou et al. 2020). One of the primary uses of epidemiology is to make it easier to identify areas and groups of people in danger and to offer the best medical and social options for reducing risk factors in such areas (Zhou et al. 2020). For 150 years, medical professionals have used maps for spatial disease analysis (WHO 2020). Anatomical epidemiology’s study of the regional distribution of infection and mortality includes geographic epidemiology (Gatto et al. 2020). Data visualization and representation as geographic maps are the first stage of analyzing geographical data (Kandwal et al. 2009). For years, GIS has extensively been modeling different diseases, businesses, the environment, and natural resources (WHO 2011). The administrators of this industry must be proficient in GIS because of the healthcare service centers’ extensive geographic reach and high activity levels. GIS’s geospatial analysis capabilities directly benefit modeling diseases’ spatial distribution and their relationships with environmental characteristics and the healthcare system. Currently, GIS technology is thought to be crucial in infectious disease study and control (Kistemann et al. 2015).

Understanding the Spatiotemporal dynamics of the prime wave of the diseases and analyzing the results of inhibitory measures have received much attention in the inquiry since Covid-19 was first reported in January 2020. In epidemiology, standard analytical and numerical models were used. For instance, Leung et al. (2020) assessed the COVID-19 immediate reproduction number and confirmed case-fatality danger in central Chinese urban and provinces, which used a Sensitive-Infectious-Recovered (SIR) model to assess the potential effects of measures following the prime wave of infection. Fanelli and Piazza’s (2020) SIR was employed to undertake a comparative analysis in China, Italy, and France. Both Danon et al. (2020) and Peixoto et al. (2020) used population models to dissect and forecast the illness extension among England and Wales, as well as the Brazilian states of So Paulo and Rio de Janeiro in the meantime, spatial statistical models were used to analyze the illness space-time dynamics. Guliyev (2020), for instance, used a spatial panel data model to study the subject of transmission dissemination in China, discovering spatial effects such as the dispensation of confirmed fatalities and recovery. To dissection

and forecast the space-time dispersion of the illness in Italy, Giuliani et al. (2020) made an endemic–epidemic multivariate time-series mixed-effects GLM for regional counts of COVID-19 confirmed.

Rahnama and Bazargan (2020) used descriptive-analytical techniques and spatial distribution modeling to investigate the spatiotemporal patterns of the COVID-19 epidemic in Iran. Their research findings revealed that the most critical geographic parameter for the COVID-19 distribution in Iran is the distance between and the vicinity of the provinces affected by the disease, which follows the pattern of the spatial distribution of adaptation. The regional distribution of COVID-19 and its fluctuation throughout the United States were modeled by Abolfazl et al. in 2020. They investigated the virus’s spread using GWR and multi-geographically weighted regression (MGWR). According to the findings of their study, GWR performs reasonably well in the spatial analysis of COVID-19 prevalence compared to the MGWR model. Pourghasemi et al. (2020) examined the COVID-19 outbreak risk indicators to pinpoint areas in Iran’s Fars region that were highly vulnerable to infection and gauge infection patterns there.

For this reason, a GIS-based machine learning system was used to evaluate the danger of a coronavirus outbreak in the province of Fars. Coronavirus infection impacts tourism and pilgrimage provinces such as Mazandaran and Qom. Qom is a pilgrimage province with many places of pilgrimage. In contrast, Mazandaran province has tourist attractions that cause heavy human traffic, contributing to a higher rate of spread in urban areas. It has been shown that citizens migrate to these provinces from different parts of Iran, which has caused the spread of the disease to dense urban areas in Iran (Patel et al. 2019). Jia et al. (2021) presented a dynamic model to describe coronavirus transmission by analyzing the relationship between virus spread and air quality conditions. They concluded that the air quality index is the most important climatic factor in virus diffusion.

Ibrahim (2020) looked at the volume and density of the risk of coronavirus pollution in Makkah, Saudi Arabia, using the GWR model. According to the findings of this study, the correlation between coronavirus pollution size and pollution density was positive, with a coefficient of 0.96. The relationship between the spatial dispersion of COVID-19 and population migration was investigated using a Bayesian spatiotemporal model during the early stage of the outbreak in Wuhan, China (Chen et al. 2020). Their investigation revealed that the Bayesian spatiotemporal model could be beneficial for rapid warning distribution and preventing the future dispersion of the virus.

Geographically weighted regression (GWR), ordinary least squares (OLS), and spatial autocorrelation (Moran’s) modeling methods are some of the most widely used in various fields of research. The spatial distribution of the

PM_{2.5} was modeled using GWR in china's cities, and the findings of this research revealed the proper functionality of this modeling approach (Gu et al. 2021). The GWR and OLS were employed in central java, Indonesia, to evaluate the impact of the human development index and population size on poverty. This study's outcomes reported good performance of these models (Mahara and Fauzan 2021). The OLS and GWR methods are used to assess the influences of geographical parameters on forming land surface temperature (Kashki et al. 2021). The results from this research exposed feasible functionalities of this modeling approach's spatial distribution of land surface temperature. Explanatory of Urban Expansion was assessed in Kolkata city using the geographically weighted regression (GWR) technique; the outputs of this study exposed the practical applicability of GWR in urban planning and management (Mondal et al. 2015). In order to investigate the effects of urbanization and landscape patterns, habitat quality (Zhu et al. 2020) employed OLS and GWR models. According to the results of this study, rapid urbanization has a significant and negative influence on habitat quality within the study area. Jiao et al. (2021) used GWR and OLS models to research the disparities in COVID-19 infections' temporally varying demographics and economic conditions, and their findings indicated the significance of the demographic and economic disparities. El Deeb (2021) used spatial autocorrelation (Moran's I) to determine the dynamic and mean center for the COVID-19 pandemic in Lebanon. The results of this investigation revealed the adoptable functionality of spatial autocorrelation in disease modeling. To evaluate the spatial distribution and relationship neighboring the regions in terms of the COVID-19 outbreak, Amaliah et al. (2021) used Moran's I Index. Considering the results of this research, a spatial autocorrelation of the confirmed cases is detected.

Following the rapid outbreak of COVID-19, public places and events, including schools and universities, movie theaters, concerts, theater shows, and national sports leagues, were closed, and office hours were decreased. Body temperature screening stations began operating at the entrance of different places. The "Stay at Home" campaign was implemented nationwide, asking people not to leave their homes to break the coronavirus transmission chain between the country's provinces and reduce social mobilization. Consequently, after a while, the government implemented the "social distancing" plan with increased active cases. Following the implementation of social distancing, the confirmed cases and mortality of coronavirus in the provinces of Qom and Mazandaran decreased. Today, the study of the distribution and pandemic diseases using modeling techniques is globally considered essential to discover the sources and conditions causing the spread of the disease in any geographical location. Since 1993, the World Health Organization (WHO) has initiated applying GIS and modeling

approaches to create disease maps. This paper intends to compare the spatiotemporal distribution of COVID-19 pandemic outbreaks utilizing the GWR model and the outcomes with the OLS model from February 24, 2020, to late October 2021, in Mazandaran and Qom provinces in Iran. This study aims to investigate the spatiotemporal distribution of COVID-19 based on three indicators (confirmed cases, deaths, and recovered) utilizing GWR and least-square models in Qom and Mazandaran provinces of Iran, from February 3, 2020, to late October 2021. Spatial autocorrelation (Global Moran's I) was used to analyze the three indicators (confirmed cases, deaths, and recovered cases).

Area of study

The study area comprises two provinces of Iran (Qom and Mazandaran). Qom province is situated between the latitudes of 34° 9" and 35° 15" N and between the longitudes of 50° 6" and 51° 58" E, sharing borders with Tehran Province to the north, Semnan Province to the east, Isfahan Province to the south and Markazi Province to the west. It has an area of 11,238 km² in the central corridor of Iran and has a population of 1.06 million (Fig. 1). Mazandaran province is located in northern Iran along the coast of the Caspian Sea, between the latitudes of 35° 45' 49", 36° 57' 42" N, and longitudes 50° 21' 5", 54° 7' 55" of E. Mazandaran province shares borders with Tehran and Qazvin in the south, Semnan to the southeast, Gilan to the west, Golestan province to the east and with Caspian Sea to the North (Fig. 1). According to the 2016 census, Mazandaran has a population of 3,283,577 (Statistical yearbook of Mazandaran Province, 2016).

Materials and methods

This study is based on secondary data, precisely information on confirmed deaths retrieved from hospitals and the National Institute of Health website for the provinces of Qom and Mazandaran between March 2, 2019, and November 30, 2021. The ALOS PALSAR digital terrain model (DTM) was acquired from (<https://search.asf.alaska.edu>). To assess the impact of elevation on the COVID-19 pandemic outbreak. The monthly average data for two chosen Iranian provinces were divided into three indicators using the Excel program (Tables 1 and 2).

Following that, in the ArcGIS 10.8.1 environment, statistical models of GWR, OLS, and spatial autocorrelation (Moran I) were employed to examine the spatiotemporal distribution of three indicators: confirmed cases, deaths, and recovered. Three indicators, confirmed cases, deaths, and recovered, were added to the research area's shapefile to implement the GWR and OLS models. The ArcGIS 10.8.1

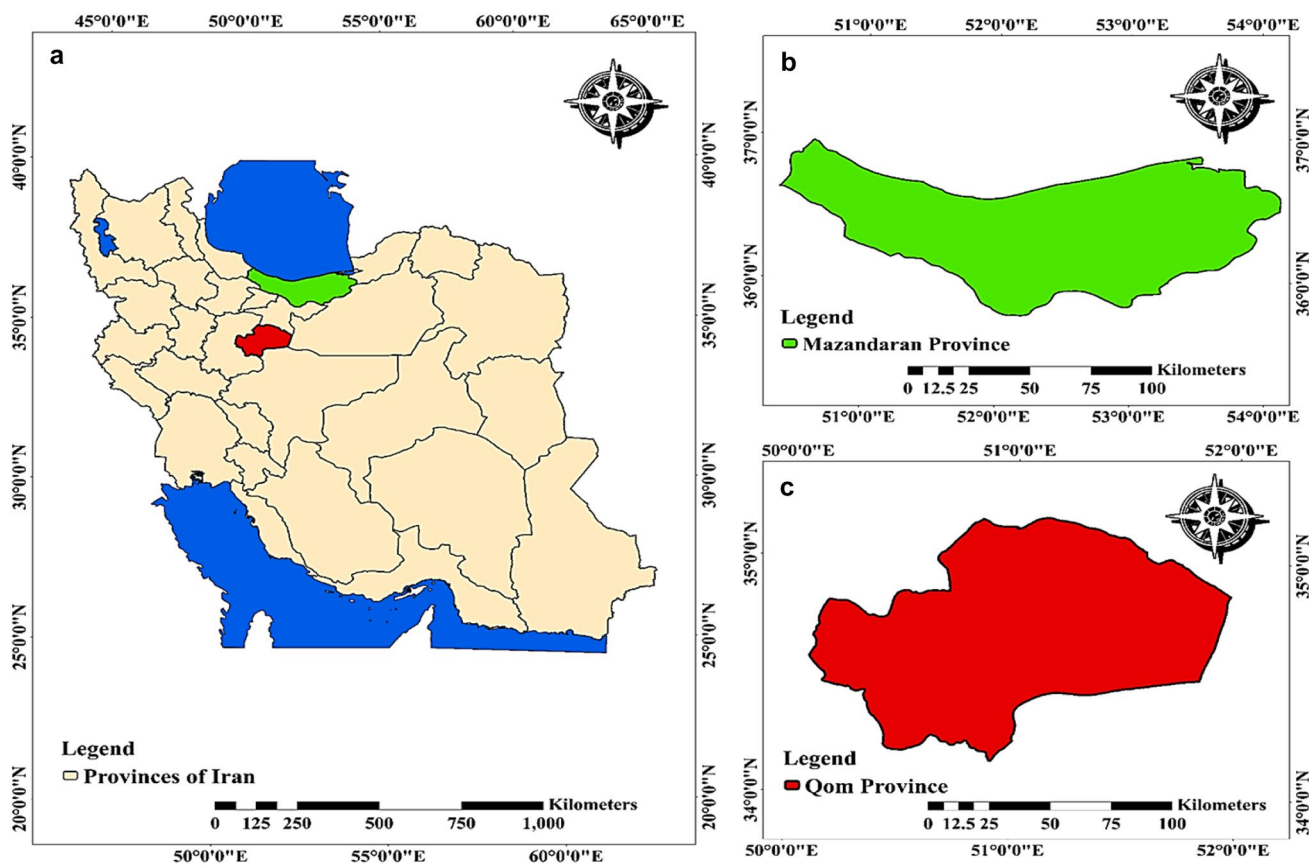


Fig. 1 Location of the study area. Provinces of Iran (A), Mazandaran province (B), and Qom province (C)

Table 1 Monthly average of COVID-19 pandemic indicators in Mazandaran province by percentage

Months	Confirmed cases	Recovered	Deaths
March	24.43	25.56	1.46
April	25.43	38.06	2.56
May	39.34	41.08	1.73
June	17.24	37.67	1.64
July	35.45	75.67	3.53
August	45.45	71.96	2.08
September	37.61	88.16	2.04
October	35.65	80.16	4.77

Table 2 Monthly average of COVID-19 pandemic indicators in Qom province by percentage

Months	Confirmed cases	Recovered	Deaths
March	35.16	25.13	4.09
April	46.13	25.25	2.01
May	48.13	21.04	1.86
June	26.41	13.04	1.36
July	46.13	21.26	2.07
August	38.03	22.03	3.04
September	66.03	38.23	3.66
October	45.73	45.83	12.66

spatial modeling module was used to develop the GWR and OLS statistical models. The shapefile of the research areas was chosen as the input for these models, and three indicators of confirmed cases, deaths, and recovered causes, were introduced to the GWR and OLS models. The spatial data for three indicators, confirmed cases, deaths, recovered cases, and a digital elevation model of the provinces of Qom and Mazandaran, are provided in (Fig. 2).

The three indicators were interpolated using the inverse distance weighting (IDW) approach to apply the GWR and OLS models. The interpolated COVID-19 pandemic indicators and digital elevation models were converted into feature polygons to suit the model implementation. An intersection overlay was employed to overlay the elevation maps and create polygons. An intersection overlay was employed to overlay the elevation maps and created polygons. Higher

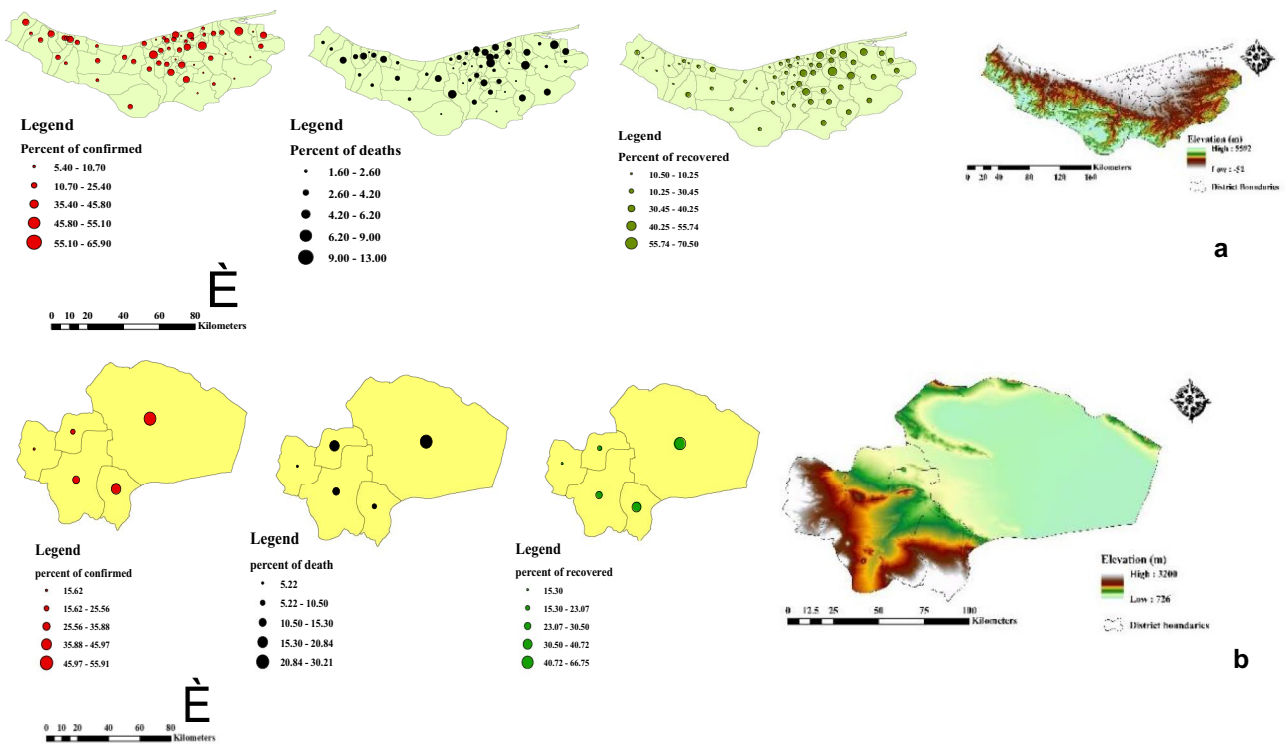


Fig. 2 Spatial data points for three indicators and digital elevation model, a Mazandaran province, b Qom province

elevation areas received higher values after the weights were added to the attribute tables.

Geographically weighted regression (GWR model)

Brunsdon et al. (1996) introduced the concept of geographically weighted regression (GWR) to the geography literature to investigate the possibility of correlations in a regression model being spatially variable, or what is known as parametric nonstationarity. GWR is based on the locally weighted regression method, established in statistics for curve-fitting and smoothing applications. The novel aspect of GWR uses a subset of data close to the model calibration point in geographic space instead of variable space. GWR is based on the non-parametric locally weighted regression approach created in statistics for curve-fitting and smoothing applications, where local regression parameters are calculated using subsets of data close to a model estimation point in variable space (Gilbert and Chakraborty 2010). The novel aspect of GWR uses a subset of data close to the model calibration point in geographic space instead of variable space (Fotheringham et al. 2002; Wang et al. 2010). GWR has been proposed as a technique to perform inference on spatially changing connections to extend the initial focus on prediction to

confirmatory analysis, while the emphasis in conventional locally weighted regression in statistics has been on curve-fitting, that is, estimating or predicting the response variable (Páez and Wheeler 2009).

Although the model calibration sites are not limited to observation locations, any observation location in the dataset may have a regression model fitted using GWR. The weights that indicate the geographical dependency between observations are calculated using the inter-point distances, which are obtained from the spatial coordinates of the data points—either individual data points or areal centroids—and then entered into a kernel function. Geographically weighted regression forms separate equations with the participation of independent and dependent variables placed inside a “distance” bar of each phenomenon and also allows parameter values to change continuously in geographic space. Equation 1 shows the GWR model (Hu et al. 2012):

$$Y_i = \beta_{i0} + \sum_1^p \beta_{ik}x_{ik} + \epsilon_i \tag{1}$$

where β_{ik} and x_{ik} are the factors and observed values of the independent variable k ($k=1, \dots, p$) for observation i ; ϵ_i is the error term for observation i .

Ordinary least squares (OLS)

One of the most famous regression analysis techniques involving identifying mechanisms operating within the real estate market is the ordinary least squares (OLS) approach (Hutcheson et al. 2019). The relationship between the dependent and independent variables can be defined by a simple straight line for which the values of y (price) are estimated by the values of x , according to the essential theoretical assumptions of the primary linear modeling method known as OLS (attributes). The predicted model must have the smallest possible sum of squares of estimated parameter errors (Deilami et al. 2016; Li et al. 2017). The fundamental issue with standard statistical analysis techniques, such as the OLS methodology, is that they typically seek to define common correlations between the variables being studied across diverse contexts (Cao et al. 2019). Through Eq. 2, the global regression model can be demonstrated:

$$Y = \beta_0 + \sum_{j=1}^p \beta_j x_j + \varepsilon \quad (2)$$

where Y is the dependent variable, β_0 is the model's intercept, X_j corresponds to the j th explanatory variable of the model ($j = 1$ to p), and ε is the random error.

Inverse distance weighting (IDW)

Inverse distance weight (IDW), a popular interpolation technique, considers that each input point has a local influence that decreases as the distance increases. The points physically closer to the processing cell are given more weight than those farther away. The output value of each location can be calculated for an analysis using IDW using either a predetermined number of points or all points inside a predetermined radius. This method's application is predicated on the idea that a variable's influence reduces as it is moved away from the spot where it was sampled (Gong et al. 2014).

The IDW technique is a moving average interpolator typically used with highly variable data. It is feasible to go back to the data collection location and record a new value for some data types that are statistically distinct from the original reading but falls within the region's overall trend. The interpolated surface is less than the maximum local value and more than the local minimum value, as determined by a moving average estimation method (Rocha et al. 2018). Through the use of Eq. 3, the inverse distance weighting algorithm is determined:

$$Z_0 = \frac{\sum_{i=1}^N z_i d_i^{-n}}{\sum_{i=1}^N d_i^{-n}} \quad (3)$$

where Z_0 is the variable estimation value, z_i is the sample value at point i , d_{iis} the distance of the sample point to the estimated point, and n is the coefficient that determines the weight based on the distance (Childs 2004).

Spatial autocorrelation (Global Moran's I)

The qualities and locations of the spatial features are addressed in the assessment of spatial autocorrelation, which considers the correlation of a variable concerning its spatial location (Goodchild 1986). A typical test statistic for spatial autocorrelation is Moran's I. When the values are distributed randomly in space, solid spatial autocorrelation occurs even though there should not be any correlation between the values. The correlation between the same values and variables in several locations is indicated by spatial autocorrelation (Global Moran's I analysis) (Lee 2011).

Moran's I value will range between -1 and 1 . A larger positive Moran's I suggest that values in nearby places tend to cluster, whereas a lower negative Moran's I suggests that high and low values are interspersed. There is no geographic autocorrelation when Moran's I is close to zero, indicating that the data are dispersed randomly (Overmars et al. 2003; Getis 2007). Equation 4 calculates it for n observations on a variable at locations i and j :

$$I = \frac{N}{W} \frac{\sum_i \sum_j w_{ij} (x_i - \bar{x})(x_j - \bar{x})}{\sum_i (x_i - \bar{x})^2} \quad (4)$$

where N is the numeral of spatial one indicator by i and j ; x is the variable of the connector; \bar{x} is the mean of x ; w_{ij} is the spatial weights matrix, and W is the sum of all.

Results

Twenty-eight confirmed cases of COVID-19 pandemic were announced on February 24, 2020, in four Provinces of Iran (Tehran, Isfahan, Markazi, and Alborz), and the confirmed cases for Qom and Mazandaran were 56.25% and 32.58% of total cases, respectively. The number of confirmed cases, recovered, and death increased from February 24, 2020, to October 2021. After Tehran, the highest number of confirmed cases infected with the COVID-19 pandemic are in Mazandaran and Qom provinces. The trend of the COVID-19 pandemic for these two Provinces (confirmed cases, recovered, and deaths) is presented in Figs. 4 and 5. The rate of confirmed cases for Qom province between February 24, 2020, and late October 2021 was 44.25%. While the rate of deaths in this province was 4.34%, the maximum spatial distribution of death cases was shown in the northwestern parts of this province.

Spatiotemporal outbreak of COVID-19 pandemic in Qom province, the GWR model

Due to pilgrimage and tourism trips to Qom province, the first case was confirmed. After February 24, 2020, the spread of the COVID-19 pandemic increased and reached more than 1000 confirmed cases in a day. Investigations from the GWR model showed that the spatial distribution of COVID – 19 is spreading in surrounding provinces increasingly via Qom, Tehran, Mazandaran, and Markazi Provinces. Consequently, the percentage of confirmed cases in Qom province is 44.25%. Most of the affected population was distributed in the southern parts of Qom province, including Nofel Loshato, Qom, and Salafchegan. Due to pilgrimage and tourism trips to Qom province, the death rate reached 4.08%. By the GWR model, most of the death cases were distributed in the northwestern and southern parts of Jafarabad, Khalajastan, and Loshato. From February 24, 2020, to late October 2021, the rate of recovered cases was 61.07%, and based on the GWR model, most of these cases are scattered in the central parts of Qom province. According to the OLS model, this province's death cases are mainly dispersed in the southwest and southern regions, the southeast, and small portions of the northwest and northeast. The OLS model's findings indicate that most recovered cases are dispersed throughout this province's northern and northwestern regions and southern cities such as Nofel Loshato, Salafchegan, and Jafarabad. Observance of health protocols, quarantine, and the closing of pilgrimage and tourism centers by the country's Health and Medical Education Organization can be the main reason for increased recovered cases. The spatiotemporal distribution of (confirmed cases, recovered, and deaths) in Qom province utilizing GWR and OLS models are presented in Fig. 6. Using the GWR model as a visual technique can reveal interesting patterns in geographic data. The spatial distribution of confirmed cases, deaths, and recovered patients in Qom province (explanatory variable) shows a strong relationship between the indicators in some provinces. The coefficient of determination (R^2), which expresses how accurate and good the model is, is one of the important parameters. This parameter is closer to 1 than other important parameters. It means that the explanatory variable can explain the changes well. This investigation exposed feasible functionalities of the GWR model in modeling the spatiotemporal distribution of the COVID-19 pandemic; according to this modeling technic, the spatial scattering of the indicators is well estimated in Qom province. Table 3 presents the results obtained from the GWR model.

In Qom province, the rate of confirmed cases and deaths are inversely related to elevation; with the increase in altitude, a considerable reduction of these two indicators can be seen. However, the rate of recovered cases in the elevated

area of this province increased significantly. Qom city, which has the lowest elevation across the Qom province (726 m), had an upward trend of deaths and confirmed cases in the whole province, while the cities of Nofel, Loshato, Salafchegan, Khalajastan, and Jafarabad, with a maximum elevation of 3200 m, exposed the lowest dispersion rate across the province. The results of the GWR model show that between February 24, 2020, and October 20, 2021, a Moran's I coefficient of 0.008821, a Z-Score of 2.230280, an expectation index value of -0.001136 , and a P value of 0.025729 were obtained. The pattern of spatial distribution (confirmed cases, recovered and death) is based on clustered spatial autocorrelation of (Moran's I), in Qom province and implies the high quantity of confirmed cases, deaths, and recovered, corresponding to the GWR model, confirmed cases, recovered, and deaths are dispersed in the southern, northwestern, and central parts of the province. However, the result of the spatial distribution of the COVID-19 pandemic obtained by employing the OLS model proved the (Moran's I) with a coefficient of 0.014834, an expectation index of 0.000871, Z-score of 3.675040 and a P value of 0.000238. Accordingly, its spatial distribution pattern is dispersed in clusters throughout the Qom province. The northern and northwestern regions of Qom are where these three COVID-19 pandemic indicators are dispersed. Spatial distribution (confirmed cases, recovered, and deaths) based on spatial autocorrelation model utilizing GWR and OLS models are presented in Fig. 7.

Spatiotemporal outbreak of COVID-19 pandemic in Mazandaran province, the OLS model

Mazandaran province is considered another province in Iran struggling with the COVID-19 pandemic and experiencing a rapid outbreak. Being the destination for the tourists of neighboring provinces is the main reason to intensify the COVID-19 pandemic outburst in this province. Figure 7 illustrates the spatiotemporal dispersion of COVID-19 pandemics in Mazandaran province applying GWR and OLS models from February 24, 2020, to October 2021.

GWR model showed that the spatial disperse of the COVID-19 pandemic from the provinces of Tehran, Qom, Gilan, Markazi, Mazandaran, and Isfahan to the adjacent regions initiated a rapid outbreak on February 24, 2020. Further spatial spread of the COVID-19 pandemic was revealed in northern, central, and northwestern regions, and the lowest incidence of the dissemination is visible in the eastern and southeastern regions of the country.

According to the outputs of the GWR model distribution of confirmed cases in Mazandaran province on February 24, 2020, was observed regularly in Ramsar, Nowshera, the southern parts of Sari, and parts of northern Babol cities. The GWR model revealed the impact of tourist trips

on the geographical dispersion of confirmed cases and the increased number of deaths in Mazandaran province. The death cases were spatially distributed mainly in the south and northern parts of Mazandaran province, including cities (Ramsar, Tonekabon, Kelardasht, Chalous, Noor, and Amol). The number of deaths in this province for February 24, 2020, to October 2021 reached 61.2%. As a result of the national COVID-19 pandemic headquarters policies, for instance, the implementation of screening, increasing the capacity of hospitals, providing accurate information about the spatial distribution of COVID-19 pandemic in Mazandaran province, and offering assistance to reduce the number of death cases, and increased recovered cases to 57.34% in north, south, and northeast parts of Mazandaran.

The rate of the spatial distribution of (confirmed cases, recovered and deaths) cases obtained by the OLS model from February 24, 2020, to October 21, 2021, is highly different from the results achieved by employing the GWR model. The result acquired utilizing the OLS model exposed confirmed cases further distributed in the central parts of Mazandaran. This dispersion caused a high number of death cases in the central parts of this province. The OLS model output indicated that, from February 24, 2020, to October 21, 2021, the cases were habitually scattered in the central parts and a small portion of the southern parts of the province. Using sanitizer and masks is considered the main factor of increment in the spatial distribution of recovered cases and potentially reduced the number of death cases in these parts of the province. Based on the OLS model, the spatial distribution of the COVID-19 pandemic needs to be better estimated. It shows that the OLS model cannot explain the COVID-19 pandemic spatial distribution epidemic in Mazandaran province. The R^2 rate for confirmed cases recovered and death is 0.72%. The outputs of the GWR model for the spatial distribution of the COVID-19 pandemic in Mazandaran are presented in Table 4 (Fig. 8).

In Table 4, residual of squares, the difference between the observed value and predicted value of the Y were acquired using the geographically weighted regression model. Relative performance measurement indicates the gamut to which the use of a statistical model causes loss of information. The threshold is the square root of the sum of the residual squares calculated for the residues. Standard deviation and low values are preferred. Coefficient of determination, how independent variables explain the viability of dependent variables. The adjusted coefficient of determination presents the measurement of the model's predictive accuracy in Table 4.

In this paper, the digital elevation model (DEM) is used to determine the effects of elevation on the spatial distribution of the COVID-19 pandemic within the specified study area. In Mazandaran Province, Chalous, Savadkooh, Ramsar, Sari, and Neka have a maximum altitude of 5599 m, and the density of the two indicators (confirmed cases and

deaths) were low. The rate of recovered cases was more significant than in the cities with lower elevations. The results show that from February 24, 2020, to late October 2021, the spatiotemporal autocorrelation of the COVID-19 pandemic based on spatial autocorrelation, with a (Moran's I) coefficient of 0.482419, an expected index value of -0.001653 , a Z-score of 106.107828, and the P value was 0%. According to this pattern, the spatial distribution of indicators (confirmed cases, deaths, and recovered) achieved by employing GWR in Mazandaran province are random. Based on the GWR model, these dispersions are primarily dispersed in this province's eastern and southeastern parts. While the spatial autocorrelation attained using the OLS model exposed a (Moran's I) coefficient equal to 0.215666, an expected index value of -0.001770 , a value of Z-score equal to 14.314292 and a P value equal to 0%. Corresponding to this model, the spatial dispersion of the patterns is a cluster-based distribution, which is observed primarily in the focus and southern parts of this province. The spatial distribution of (confirmed, death, and recovered) cases of the COVID-19 pandemic according to spatial autocorrelation patterns utilizing GWR and OLS is demonstrated in Fig. 9.

Discussion

Overall, our research results show the exponential growth of mortality in the central regions of Qom and Mazandaran and the quick dispersion of this virus compared to other regions. Other studies have also been performed about two widespread diseases and COVID-19, and the bulk showed an affirmative relationship between patients with COVID-19 and other diseases, such as blood pressure, diabetes, and cardiovascular diseases (Guan et al. 2020; Li et al. 2020). An analysis of COVID-19 and the number of deaths using modeling tools was shown in prior research to involve a wide range of socioeconomic and environmental parameters (Smith and Mennis 2020). In addition, Giuliani et al. (2020) also modeled the spatiotemporal dynamics of outbreaks and mortality due to COVID-19 at the provincial level in Italy. The local pandemic was more diverse than it was in Italy. Although it had a solid northward bias, it was slowly making its way into the southern provinces. The spatial distribution of the COVID-19 pandemic with the GWR model revealed the highest rate of deaths in the northwestern and southern parts of Jafarabad and Khalajistan cities and the city of Nofel Loshato during February 24, 2020, to late October 2021. During these 8 months, Qom province's recovery rate reached 61.6%. Most of these cases were observed in the central parts of this province based on the GWR model (Fig. 3). The results are similar to the results of research conducted by (Xu et al. 2022) to evaluate influencing factors of

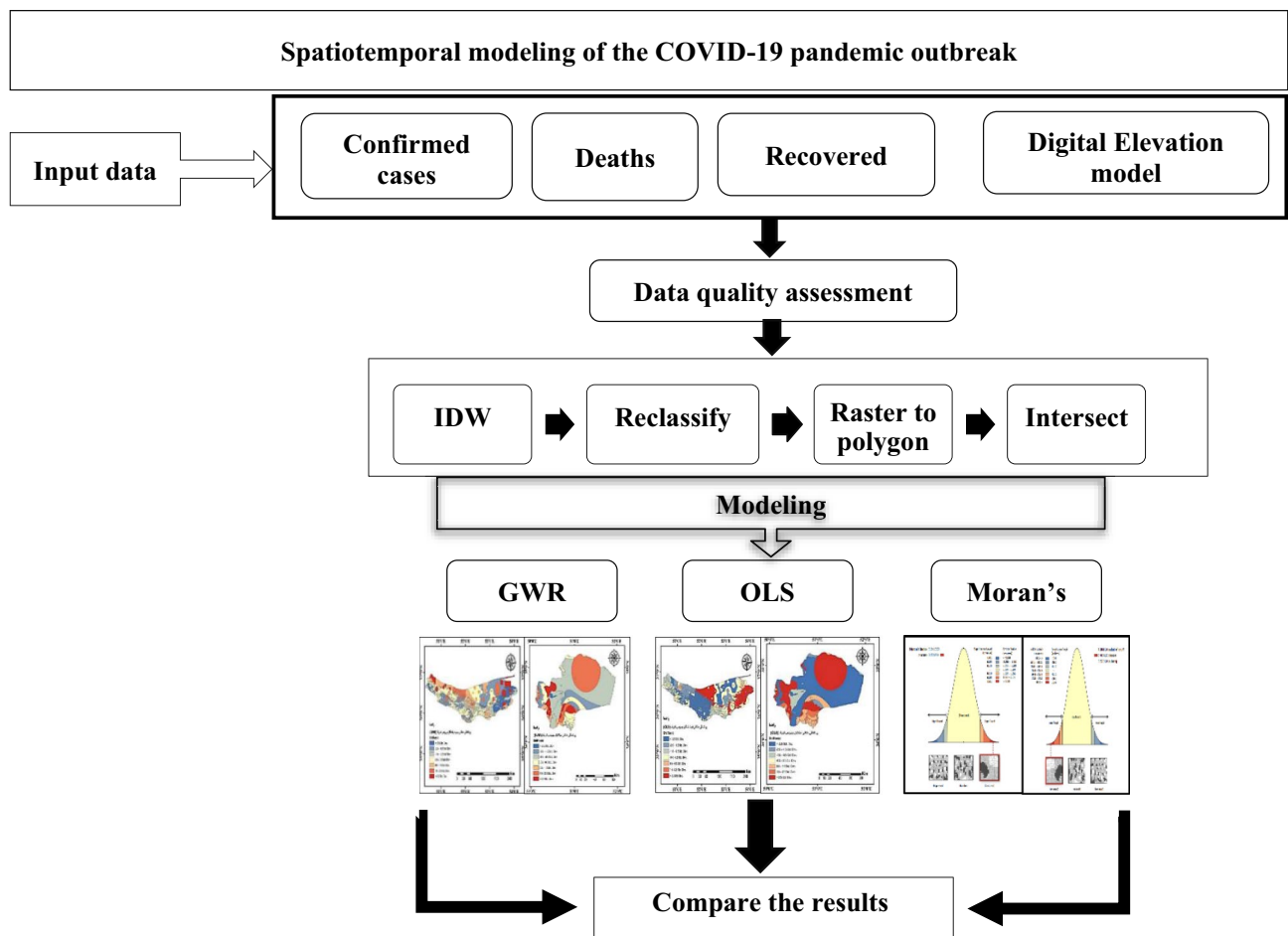


Fig. 3 Workflow of the methodology

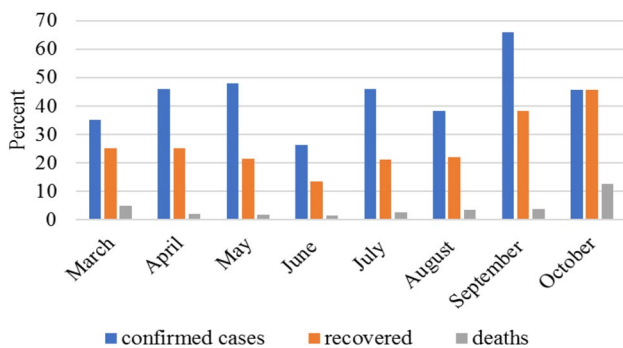


Fig. 4 Average of three indicators of the COVID-19 pandemic in Qom province

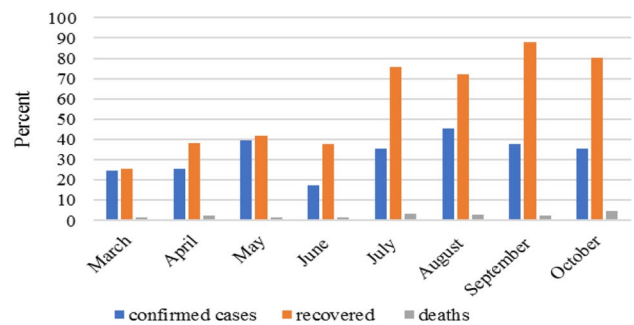


Fig. 5 Average three indicators of the COVID-19 pandemic in Mazandaran province

self-reported COVID-19 dispersion using GWR and OLS models in Wuhan, China. Xu et al. (2022) stated the feasible functionalities of OLS and GWR models in the spatiotemporal modeling of pandemic disease. However, the OLS model exposed a different spatial distribution of the COVID-19 pandemic. In addition, the results of research

conducted in order to study the propagation of the virus, Abolfazl et al. (2020) used GWR and multi-geographical weighted regression (MGWR) to predict the prevalence of (COVID-19) geographically as well as its variability across the United States. Compared to the MGWR model, findings of this study showed that GWR performed relatively well in the spatial analysis of COVID-19 prevalence.

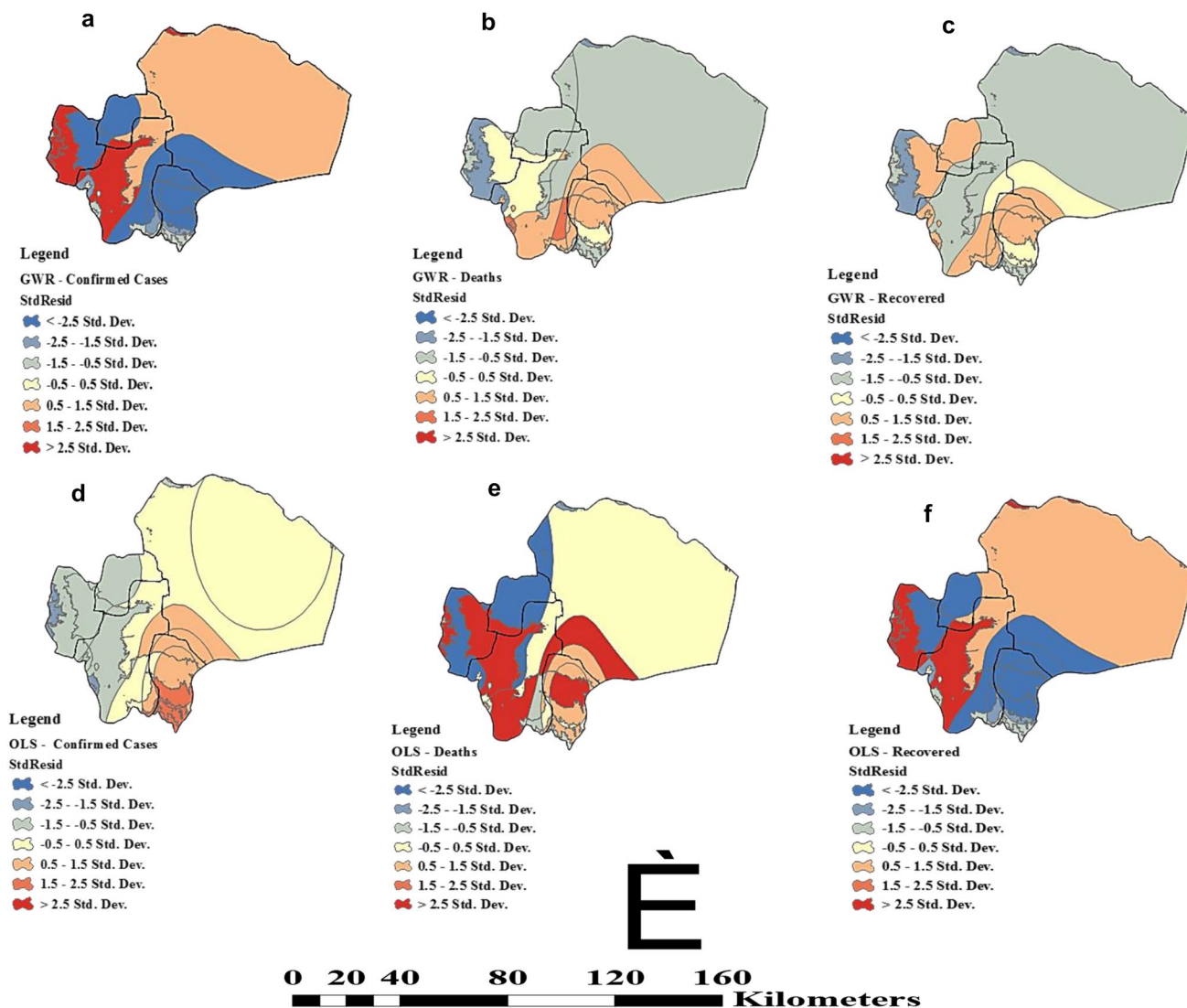


Fig. 6 Spatiotemporal distribution of COVID-19 pandemic utilizing GWR (a, b, c) and OLS (d, e, f) model

According to the OLS model, confirmed cases in Qom province are generally scattered in Khalajistan, the south-east of Nofel Loshato, and parts of the south of Salafchegan cities. Considering the results of the OLS model,

Table 3 The GWR model for indicators (confirmed cases, recovered, and death) in Qom province

Records	Parameters	Amount of parameters
1	The residual of least squares	34.15
2	Relative performance measurement	0.81
3	Threshold	15.76
4	R^2	70.41
5	R^2 (adjusted)	50.40

confirmed cases are dispersed in central and southern parts of Mazandaran province. As a result of the spatial dispersion, the central regions exposed the most significant number of death cases. As a result, this condition led to the National COVID-19 pandemic Headquarters policies, such as implementing the screening plan and increasing the capacities of the hospitals.

Regarding the outputs of the GWR model, after implementing these policies, the rate of deaths and confirmed cases were mitigated and recovered evidence increased significantly by 57.34% in the north, south, and northeast regions of Mazandaran province. Peak et al. (2020) demonstrated the impacts of quarantine on the rate of COVID-19 dispersion and deaths.

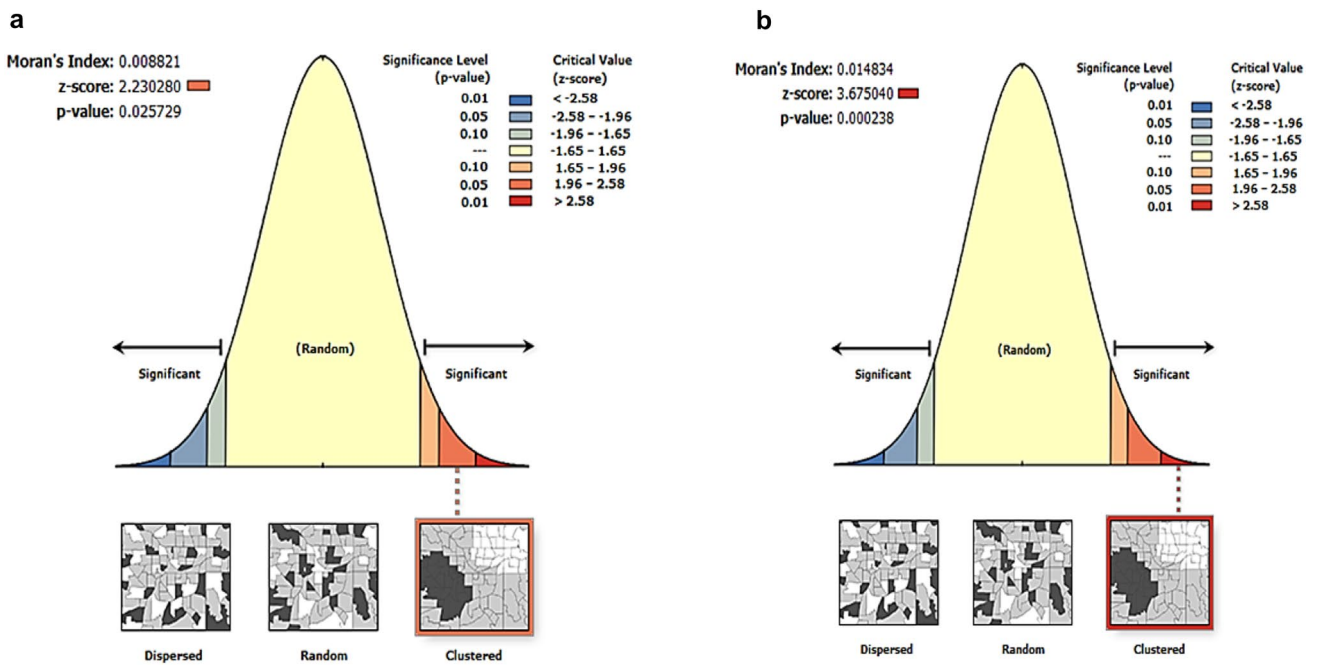


Fig. 7 Spatial distribution of (confirmed cases, deaths, and recovered) cases obtained using a GWR and b OLS model

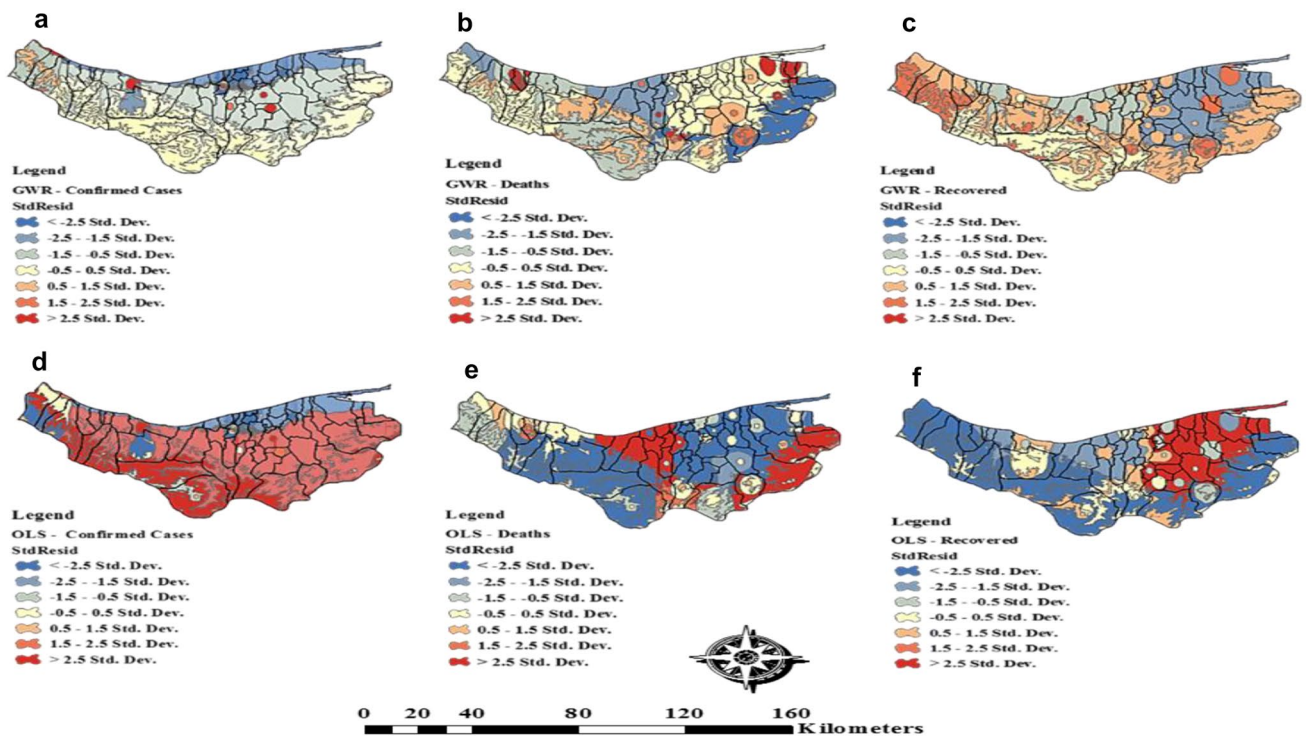


Fig. 8 Spatiotemporal distribution of COVID-19 pandemic utilizing GWR (a, b, c) and OLS (d, e, f) model

Table 4 Results obtained from the GWR model for indicators (confirmed cases, deaths, and recovered) in Mazandaran province

Records	Parameters	Amount of parameters
1	The residual of least squares	51.25
2	Relative performance measurement	66.96
3	Threshold	59.15
4	R^2	0.72
5	R^2 (adjusted)	71.69

Conclusion

The prevalence of the COVID-19 pandemic has come to be a clinical threat all over the world. According to the results of this research, the models (GWR, OLS, and Moran’s I) used in this study exposed adequate capabilities to investigate the spatiotemporal variation of pandemic disease and quantify the influences of explanatory factors. According to the outputs of GWR, the spatial distribution of the COVID-19 pandemic in Qom province is very well estimated. It shows that the GWR model could explain the pandemic of COVID-19 spatial distribution in Qom province confirmed cases, recovered, and death rate $R^2 = 70.41\%$. Moreover, outputs of the GWR model for Mazandaran province revealed that the confirmed cases in this province are generally witnessed in Ramsar, Nowshahr, and the southern parts of Sari, the northern region of Babol influenced by tourists’ trips and transportation. Based on the GWR model, the highest spatial

distribution of deaths, with a percentage of 2.61%, is observed in the northwestern and southern parts (Ramsar, Tonekabon, Kelardasht, Chalous, Noor, and Amol) in Mazandaran province.

Moreover, the outputs of the OLS model exhibited that the death cases in Qom province mainly depressed in the southwestern and southern parts and part of the southeast and a small region of the northwest and northeast, and the recovered cases are observed in northern, northwestern, and eastern areas. Based on the OLS model, the spatial distribution of the COVID-19 pandemic is not well estimated compared to GWR. It shows that the OLS model has not been able to explain the COVID-19 pandemic spatial distribution epidemic in Mazandaran province. According to the outcomes of this model, the R^2 for confirmed cases recovered and death is 0.72%. The findings of the GWR model demonstrate that the COVID-19 pandemic’s spatial-temporal autocorrelation was based on spatial autocorrelation, with a Moran’s I coefficient of 0.482419, an expected index value of -0.001653 , a Z-score of 106.107828, and a P value of 0%.

While the spatial autocorrelation attained using the OLS model in Mazandaran province exposed a (Moran’s I) coefficient equal to 0.215666, an expected index value of -0.001770 , a value of Z-score equal to 14.314292 and a P value equal to 0%.

The results of this paper in Mazandaran and Qom Provinces indicated that the indicators of confirmed cases and deaths are inversely related to the altitude, and the rate of recovered cases has a direct relationship with the elevation.

Based on Moran’s autocorrelation pattern, the results of the GWR model confirmed that a coefficient of 0.008821

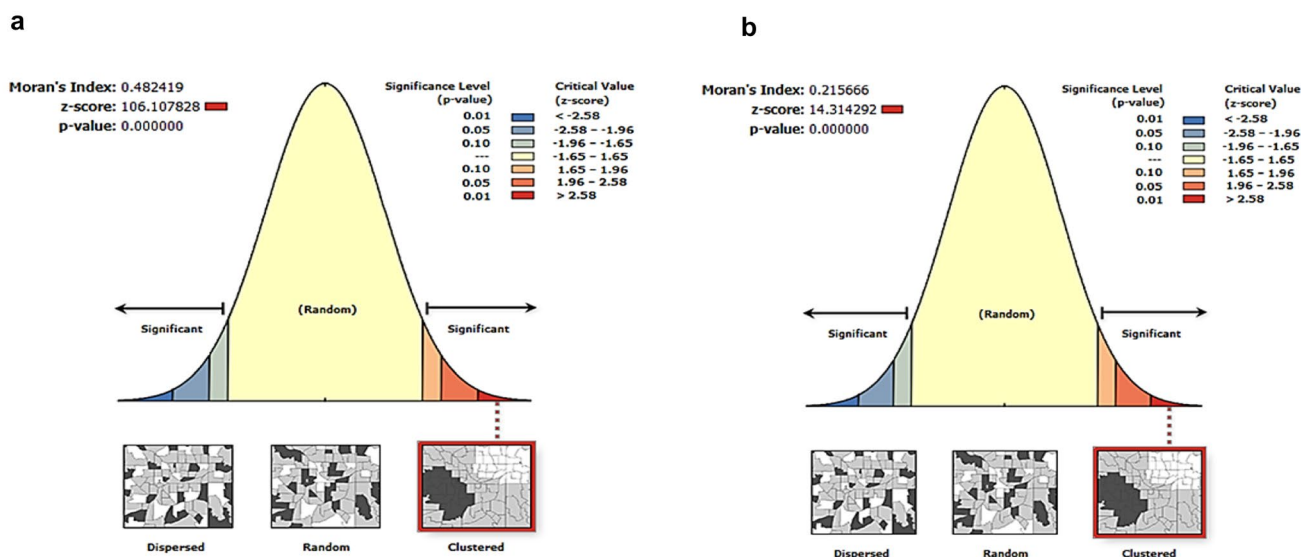


Fig. 9 Spatial distribution of (confirmed, deaths, and recovered) cases obtained using **a** GWR and **b** OLS model

for (Moran's I), 2.230280 for Z-Score, the value of the expectation index being -0.001136 and the P value equal to 0.025729% are acquired, while the result of the spatial distribution of the COVID-19 epidemic obtained using the OLS model showed a coefficient (Moran's I) of 0.014834, an expectation index of 0.000871, a Z-score of 3.675040 and a P value of 0.000% for Qom province. Wearing masks and using sanitizers are considered the most critical factors in reducing deaths. A significant increase in recovered cases decreases the number of deaths and increases the rate of recovered cases in Mazandaran.

Author contributions The authors thank the reviewers for evaluating the article.

Funding The research does not receive any funding.

Data availability The available data for this paper are available at the following sites: (1) Monthly and annual counts of cases, deaths, and recurrences of the COVID-19 pandemic based on Iran's provinces exist from the Ministry of Health of Iran website at the following address. <https://behdasht.gov.ir/>. (2) Digital elevation model of 12.5 m' height for the two provinces of Qom and Mazandaran from the website. <https://search.asf.alaska.edu/>.

Declarations

Conflict of interest The authors have no conflict of interest.

Ethical approval Not applicable.

Consent for publication Not applicable.

References

- Abolfazl M, Behzad V, Kiara MR (2020) GIS-based spatial modeling of COVID-19 incidence rate in the continental United States. *Sci Total Environ*. <https://doi.org/10.1016/j.scitotenv.2020.138884>
- Amaliah ON, Sukmawaty Y, Susanti DS (2021) Spatial autocorrelation analysis of Covid-19 cases in South Kalimantan Indonesia. *J Phys*. <https://doi.org/10.1088/1742-6596/2106/1/012005>
- Bailley T, Gatrell A (2015) *Interactive spatial data analysis*, 1st edn. Longman, Harlow
- Brunsdon C, Fotheringham AS, Charlton M (1996) Geographically weighted regression: a method for exploring spatial nonstationarity. *Geogr Anal* 28(4):281–298
- Cao K, Diao M, Wu B (2019) A big data-based geographically weighted regression model for public housing prices: a case study in Singapore. *Ann Am Assoc Geogr* 109:173–186. <https://doi.org/10.1080/24694452.2018.1470925>
- Chen N, Zhou M, Dong X, Qu J, Gong F, Han Y (2020) Epidemiological and clinical characteristics of 99 cases of 2019 novel coronavirus pneumonia in Wuhan, China, a descriptive study. *Lancet* 39:507–513. [https://doi.org/10.1016/S0140-6736\(20\)30211-7](https://doi.org/10.1016/S0140-6736(20)30211-7)
- Childs C (2004) Interpolating surfaces in ArcGIS spatial analyst. *ArcUser* 3235(569):32–35
- Comito C, Pizzuti C (2022) Artificial intelligence for forecasting and diagnosing COVID-19 pandemic: a focused review. *Artif Intell Med*. <https://doi.org/10.1016/j.artmed.2022.102286>
- Danon L, Bailey M, Keeling M, A Spatial Model of CoVID-19 Transmission in England and Wales: Early Spread and Peak Timing. *MedRxiv*. doi:, de Jong P, Sprenger C (2020) and F. Van Veen. 1984
- Deilami K, Kamruzzaman M, Hayes JF (2016) Correlation or causality between land cover patterns and the urban heat island effect? Evidence from Brisbane, Australia. *Remote Sens* 8(9):716
- El Deeb O (2021) Spatial autocorrelation and the dynamics of the mean center of COVID-19 infections in Lebanon. *Front Appl Math Stat*. <https://doi.org/10.3389/fams.2020.620064>
- Fanelli D, F P (2020) Analysis and forecast of COVID-19 spreading in China, Italy and France. *Chaos Solit Fractals* 134:109761. <https://doi.org/10.1016/j.chaos.2020.109761>. (Online in ScienceDirect)
- Fotheringham AS, Brunsdon C, Charlton M (2002) *Geographically weighted regression: the analysis of spatially varying Relationships*. Wiley, Chichester
- G Hutcheson (2019) *GLM models and OLS regression*. The University of Manchester, Manchester
- Gatto M, Bertuzzo E, Mari L, Miccoli S, Carraro L, Casagrandi R, Rinaldo A (2020) Spread and dynamics of the COVID-19 epidemic in Italy: effects of emergency containment measures. *Proc Natl Acad Sci USA* 1(17):10484–10491
- Getis A (2007) Reflections on spatial autocorrelation. *Reg Sci Urban Econ* 37(4):491–496. <https://doi.org/10.1016/j.regsciurbeco.2007.04.005>
- Gilbert A, Chakraborty J (2010) Using geographically weighted regression for environmental justice analysis: cumulative cancer risks from air toxics in Florida. *Soc Sci Res* 40(1):273–286
- Giuliani D, Dickson MM, Espa G, Santi F (2020) Modelling and predicting the spatio-temporal spread of coronavirus disease 2019 (COVID-19) in Italy. *BMC Infect Dis Vol*. <https://doi.org/10.2139/ssrn.3559569>. (SSRN Electronic Journal)
- Giuliani D, Dickson M, Espa G, Santi F (2020) Modelling and predicting the spread of coronavirus (COVID-19) infection in NUTS-3 Italian regions. *arXiv Preprint.arXiv: 2003.06664*
- Gong G, Mattevada S, Bryant S (2014) Comparison of the accuracy of kriging and IDW interpolations in estimating groundwater arsenic concentrations in Texas. *Environ Res* 130(0):59–69
- Goodchild MF (1986) *Spatial autocorrelation*; CATMOG 47, Geo-books: Norwich, UK
- Gu K, Zhou Y, Sun H, Dong F, Zhao L (2021) Spatial distribution and determinants of PM2.5 in China's cities: fresh evidence from IDW and GWR. *Environ Monit Assess*. <https://doi.org/10.1007/s10661-020-08749-6>
- Guan WJ, Liang WH, Zhao Y, Liang HR, Chen ZS, Li YM, He JX (2020) A nationwide analysis of comorbidity and its impact on 1590 patients with COVID-19 in China. *Eur Respir J*. <https://doi.org/10.1183/13993003.00547-2020>
- Guliyev H (2020) Determining the spatial effects of COVID-19 using the spatial panel data model. *Spatial Stat* 38:100443 <https://doi.org/10.1016/j.spasta.2020.100443> (Online in ScienceDirect)
- Hu G, Li ZJ, Wang JF (2012) Determinants of hand, foot, and mouth disease incidence in China using geographically weighted regression models. *PLoS One* 7(6):e38978
- Ibrahim A (2020) GIS application for modeling Covid-19 risk in the makkah region Saudi risk Arabia based on population and density. *Egypt J Environ Change*. <https://doi.org/10.21608/ejec.2020.115873>
- Jia J, Ding J, Liu S, Liao G, Li J, Duan B (2021) Modeling the control of COVID-19, impact of policy interventions and meteorological factors. 151:231–3217
- Jiao J, Chen Y, Azimian A (2021) Exploring temporal varying demographic and economic disparities in COVID-19 infections in four U.S. areas: based on OLS, GWR, and random forest models. *Comput Urban Sci* 1(1):1–16. <https://doi.org/10.1007/s43762-021-00028-5>

- Kandwal R, Garg PK, Garg RD (2009) Health GIS and HIV/ AIDS studies: perspective and retrospective. *J Biomed Inf* 4(2):748–755. <https://doi.org/10.1016/j.jbi.2009.04.008>
- Kashki A, Karami M, Zandi R, Roki Z (2021) Evaluation of the effect of geographical parameters on the formation of the land surface temperature by applying OLS and GWR, a case study Shiraz City. *Iran Urban Clim* 37(March):100832. <https://doi.org/10.1016/j.uclim.2021.100832>
- Kistemann T, Dangendorf F, Schweikart J (2015) New perspectives on the use of geographical information systems in environmental health sciences. *Int J Hyg Environ Health* 20(5):169–181. <https://doi.org/10.1078/1438-4639-00145>
- Lee KH (2011) Integrating carbon footprint into supply chain management: the case of Hyundai Motor Company (HMC) in the automobile industry. *J Clean Prod* 19(11):1216–1223
- Leung K, Wu J, Liu D, Leung G (2020) First-wave COVID-19 transmissibility and severity in China outside Hubei after control measures, and second-wave scenario planning: a modelling impact assessment. *Lancet* 395(10233):1382–1393. [https://doi.org/10.1016/S0140-6736\(20\)30746-7](https://doi.org/10.1016/S0140-6736(20)30746-7)
- Li X, Zhou Y, Asrar GR, Imhoff M, Li X (2017) The surface urban heat island response to urban expansion: a panel analysis for the conterminous United States. *Sci Total Environ* 605:426–435
- Li W, Thomas R, El-Askary H, Piechota T, Struppa D, Ghaffar KAA (2020) Investigating the significance of aerosols in determining the coronavirus fatality rate among three European countries. *Earth Syst Environ*. <https://doi.org/10.1007/s41748-020-00176-4>
- Lu R, Zhao X, Li J, Niu P, Yang B, Wu H (2020) Genomic characterization and epidemiology of 2019 novel corona virus: implications for virus origins and receptor binding. *Lancet* 39(5):565–574. [https://doi.org/10.1016/S0140-6736\(20\)30251-8](https://doi.org/10.1016/S0140-6736(20)30251-8)
- Mahara DO, Fauzan A (2021) Impacts of human development index and percentage of total population on poverty using OLS and GWR models in Central Java, Indonesia. *EKSAKTA J Sci Data Anal* 2(2):142–154. <https://doi.org/10.20885/eksakta.vol2.iss2.art8>
- Mollalo A, Vahedi B, Rivera K (2020) GIS-based spatial modeling of COVID-19 incidence rate in the continental United States. *Sci Total Environ* 728:1–8. <https://doi.org/10.1016/j.scitotenv.138884>
- Mondal B, Das DN, Dolui G (2015) Modeling spatial variation of explanatory factors of urban expansion of Kolkata: a geographically weighted regression approach. *Model Earth Syst Environ* 1(4):1–13. <https://doi.org/10.1007/s40808-015-0026-1>
- Overmars KP, de Koning GHJ, Veldkamp A (2003) Spatial autocorrelation in multi-scale land use models. *Ecol Model* 164(2–3):257–270. [https://doi.org/10.1016/s0304-3800\(03\)00070-x](https://doi.org/10.1016/s0304-3800(03)00070-x)
- Páez A, Wheeler DC (2009) Geographically weighted regression. *International Encyclopedia of Human Geography*. Elsevier, Oxford (**In press**)
- Patel H, Parikh S, Patel A, Parikh A (2019) An application of ensemble random forest classifier for detecting financial statement manipulation of Indian listed companies. In: Kalita J, Balas V, Borah S, Pradhan R (eds) *Recent developments in machine learning and data analytics. Advances in intelligent systems and computing*. Springer, Singapore, p 740. https://doi.org/10.1007/978-981-13-1280-9_33
- Peak CM, Kahn R, Grad YH, Childs LM, Li R, Lipsitch M, Buckee CO (2020) Individual quarantine versus active monitoring of contacts for the mitigation of COVID-19: a modelling study. *Lancet Infect Dis* 20(9):1025–1033. [https://doi.org/10.1016/S1473-3099\(20\)30361-3](https://doi.org/10.1016/S1473-3099(20)30361-3)
- Peixoto PD, Marcondes C, Peixoto L, Queiroz R, Gouveia A, Delgado Oliva S (2020) Potential dissemination of epidemics based on Brazilian mobile geolocation data part I: population dynamics and future spreading of infection in the States of Sao Paulo and Rio De Janeiro during the pandemic of COVID-19. *medRxiv*. <https://doi.org/10.1101/2020.04.07.20056739>
- Pourghasemi HR, Pouyan S, Heidari B, Farajzadeh Z, Fallah Shamsi SR, Babaei S, Khosravi R, Etemadi M, Ghanbarian G, Farhadi A, Safaeian R, Heidari Z, Tarazkar MH, Tiefenbacher JP, Azmi A, Sadeghian F (2020) Spatial modeling, risk mapping, change detection, and outbreak trend analysis of coronavirus (COVID-19) in Iran (days between February 19 and June 14, 2020). *Int J Infect Dis* 98:90–108. <https://doi.org/10.1016/j.ijid.2020.06.058>
- Rahnama MR, Bazargan M (2020) Analysis of spatio-temporal patterns of Covid 19 virus epidemic and its risks in Iran. *J Environ Risk Manag* 7(2):127–113
- Rocha Á, Adeli H, Reis LP, Costanzo S (eds) (2018) *Trends and advances in information systems and technologies*. 1
- Smith CD, Mennis J (2020) Incorporating geographic information science and technology in response to the COVID-19 pandemic. *Prev Chronic Dis*. <https://doi.org/10.5888/pcd17.200246>
- Wang J, Liu X, Christakos G (2010) Assessing local determinants of neural tube defects in the Heshun Region, Shanxi Province, China. *BMC Public Health* 10:52
- World Health Organization (2011) 10 facts on neglected tropical diseases. Available from: URL: https://www.who.int/features/factfiles/neglected_tropical_diseases/en
- World Health Organization (2020) Report of the WHO-China joint mission on coronavirus disease 2019 (COVID-19). Retrieved from <https://www.who.int/docs/defaultsource/coronaviruse/who-china-joint-missiononcovid-19-final-report.pdf>.
- Wu F, Chen YM, Wang W, Song Z, Hu Y (2020) A new corona virus associated with human respiratory disease in China. *Nature*. <https://doi.org/10.1038/s41586-020-2202-3>
- Xu G, Jiang Y, Wang S, Qin K, Ding J, Liu Y, Lu B (2022) Spatial disparities of self-reported COVID-19 cases and influencing factors in Wuhan, China. *Sustain Cities Soc* 76:103485. <https://doi.org/10.1016/j.scs.2021.103485>
- Zhou P, Yang L, Wang G, Hu B, Zhang L, Zhang W (2020) A pneumonia outbreak associated with a new corona virus of probable bat origin. *Nature* 5(21):270–273
- Zhu C, Zhang X, Zhou M, He S, Gan M, Yang L, Wang K (2020) Impacts of urbanization and landscape pattern on habitat quality using OLS and GWR models in Hangzhou, China. *Ecol Ind* 117(May):106654. <https://doi.org/10.1016/j.ecolind.2020.106654>

Publisher's Note Springer Nature remains neutral with regard to jurisdictional claims in published maps and institutional affiliations.

Springer Nature or its licensor (e.g. a society or other partner) holds exclusive rights to this article under a publishing agreement with the author(s) or other rightsholder(s); author self-archiving of the accepted manuscript version of this article is solely governed by the terms of such publishing agreement and applicable law.

Authors and Affiliations

Vahid Isazade¹ · Abdul Baser Qasimi²  · Pinliang Dong³ · Gordana Kaplan⁴ · Esmail Isazade⁵

Vahid Isazade
vahidisazade75@gmail.com

Pinliang Dong
pinliang.dong@unt.edu

Gordana Kaplan
kaplangorde@gmail.com

Esmail Isazade
ismailisazadeh75@gmail.com

¹ Department of Geographical Sciences, Khwarazm University, Tehran, Iran

² Department of Geography, Education Faculty, Samangan University, Samangan, Afghanistan

³ Department of Geography and the Environment, University of North Texas, 1155 Union Circle, Denton #305279, TX 76203, USA

⁴ Institute of Earth and Space Sciences, Eskisehir Technical University, Eskişehir, Türkiye

⁵ Department of Urban planning, Kharazmi University, Tehran, Iran